JTTEE5 16:913–918
DOI: 10.1007/s11666-007-9105-9
1059-9630/$19.00 © ASM International

Fuzzy Logic Analysis of Alumina-Titania Deposition Yield During APS Process

Abdoul-Fatah Kanta, Ghislain Montavon, Marie-Pierre Planche, and Christian Coddet

(Submitted February 27, 2007; in revised form May 21, 2007)

The behavior modeling of Atmospheric Plasma Spray (APS) process requires a global approach which considers interrelated non-linear relationships between coating characteristics/properties in-service and process parameters (power, feedstock injection, kinematics, etc.). Such an approach would permit to reduce the development costs. To reach this objective, the knowledge of the interactions between process parameters plays a relevant role in the optimization. This work intends to develop a behavior model based on fuzzy logic concepts. Here, the model considers the deposition yield as the result of the process and it establishes relationships with power process parameter (arc current intensity, plasma gas total flow rate, hydrogen content) on the basis of fuzzy rules. The model hence permits to discriminate the role and the effects of each power process parameters. The modeling results are compared to experimental data. The specific case of the deposition of alumina-titania (Al_2O_3-TiO_2, 13% by weight) by Atmospheric Plasma Spraying (APS) is considered.

Keywords properties of coatings, spray deposition, APS coatings, diagnostics and control

1. Introduction

Atmospheric Plasma Spraying (APS) is a technology aiming at producing coatings of thicknesses ranging from about 100 μm up to a few millimeters onto mechanical components to confer them specific and unique functional properties, such as wear and corrosion resistances, friction coefficient adaptation, thermal and electrical insulation, biocompatibility, repair, etc. (Ref 1). During this complex process, a rapid sequence of events occurs, including particle melting (and eventually also partial vaporization), particle impact and spreading onto the substrate or previously deposited layers and particle solidification to form lamellae (Ref 2). In APS, the result (i.e., the coating properties in service resulting principally but not exclusively from its structure) is indirectly linked to the selection of the operating parameters. To ensure the reproducibility of coatings of high quality, it is necessary to understand the physical phenomena during the plasma spray process.

Modeling and analysis of plasma spray processes have become increasingly important thanks to the large acceptance of concepts such as hierarchical control and factory automation. However, these processes are rendered more complicated by many interactions between their operating parameters such as deadlock, conflict, as well as uncertainties in the manufacturing environment such as tool changes or variability in production requirements. Numerous works were dedicated to establish correlations between processing parameters and in-flight particle characteristics or coating structure and properties (Ref 3, 4). Artificial intelligence computation proved to be a pertinent optimization tool permitting to take into account the non-linear characters of the correlations occurring in thermal spraying (Ref 5).

This article intends to develop a model-based estimation for the power process parameters in the APS process. An estimation scheme, which is based on fuzzy logic, is proposed to predict the yield deposition (i.e., the deposited thickness per pass of the torch in front of the part to be coated) as a function of the arc current intensity, the plasma gas total flow rate and the hydrogen content. Experimental data are used to define the data rule. In turn, these rules permit to predict the deposition yield. Alumina-titania coatings were processed and the thickness was measured for various power process parameters.

2. Experimental Procedures

The experimental step permitted to develop a database in order to evaluate the effect of selected power process parameters on deposition yield. Also, this experimental database was used to validate the fuzzy logic computational results.

This article is an invited paper selected from presentations at the 2007 International Thermal Spray Conference and has been expanded from the original presentation. It is simultaneously published in *Global Coating Solutions, Proceedings of the 2007 International Thermal Spray Conference*, Beijing, China, May 14-16, 2007, Basil R. Marple, Margaret M. Hyland, Yuk-Chiu Lau, Chang-Jiu Li, Rogerio S. Lima, and Ghislain Montavon, Ed., ASM International, Materials Park, OH, 2007.

Abdoul-Fatah Kanta, Marie-Pierre Planche, and **Christian Coddet**, LERMPS, UTBM, Belfort 90010, France; and **Ghislain Montavon**, SPCTS, UMR CNRS 6638, Université de Limoges, Limoges Cedex 87060, France. Contact e-mail: abdoul-fatah.kanta@utbm.fr.

Metco 130 (Sulzer-Metco, Rigackerstrasse 16, 5160 Wohlen, Switzerland) fused and crushed grey alumina (Al_2O_3-TiO_2, 13% by weight) powder was selected as the feedstock powder.

Thick coatings were produced onto button-type AISI 304L (stainless steel) samples of 25 mm diameter and 20 mm thick. Prior to spraying, samples were degreased by immersion in alcohol (ethanol) vapors and manually grit-blasted using white corundum (α-Al_2O_3) of average diameter of 250 μm. After grit-blasting, surfaces to be coated presented an average roughness of about 3 μm.

Sulzer F4-type atmospheric plasma torch (Sulzer-Metco, Rigackerstrasse 16, 5160 Wohlen, Switzerland) of 50 kW maximum operating power equipped with a 6 mm internal diameter anode nozzle was selected to carry out the experiments. The feedstock carrier gas flow rate was fixed at 3.2 SLPM; indeed, it did not appear necessary to adjust the carrier gas flow rate during the experiments when varying the power parameters in the considered range to keep an ''optimal particle trajectory'' because the particle trajectory remaining almost identical. The injection distance from the injector tip to the torch centerline axis was 6 mm, injector internal diameter was 1.8 mm, feedstock rate was 22 g mn^{-1}, scanning step was 12 mm per pass and spray distance was 125 mm (with a normal spray angle).

The deposition yield represents the average thickness deposited per pass. It is usually estimated using a micrometer caliper. However, more accurate results can be obtained by image analysis measurements. The coating average thicknesses were measured by the protocol depicted in Ref 6 and the deposition yield is the ratio of the average coating thickness to the number of passes. Several sets of power operating parameters were defined to manufacture the coatings. These sets permitted to study the effects of the arc current intensity, the plasma gas total flow rate and the hydrogen fraction. Table 1 lists extensively the operating parameter sets and the resulting experimentally measured deposition yields.

2.1 Arc Current Intensity

The effect of the arc current intensity was addressed between 350 and 750 A by fixing the hydrogen ratio and the plasma gas total flow rate at 35% and 54 SLPM, respectively. It is unambiguous that the arc current intensity permits to increase the deposition yield.

2.2 Plasma Gas Total Flow Rate

The impact of this parameter was studied over the 30-70 SLPM range by keeping the hydrogen ratio and the arc current intensity constant at 35% and 530 A, respectively. From a general point of view, the deposition yield decreases as the plasma gas total flow rate increases (due to a decrease in the particle residence time in the plasma flow, the particle heating is decreased and only a narrower fraction of the particle size distribution forms the coating).

2.3 Hydrogen Ratio

The effect of this parameter on the deposition yield was studied between 0 and 50%, whereas the plasma gas total flow rate and the arc current intensity were kept constant at 54 SLPM and 530 A, respectively. The variation of this parameter presents a marked effect on the yield deposition, similar to that of the arc current intensity.

From these investigations, the two prevalent parameters, which make possible to increase the average deposition yield, are the hydrogen ratio and the arc current intensity (Table 1). Indeed, these two parameters mainly influence the plasma jet enthalpy and thus it is capable to melt an increasingly broader fraction of the particle size distribution of the injected feedstock.

3. Fuzzy Logic Method

In this study, fuzzy logic (FL) concept is implemented to predict the deposition yield by varying the three considered power-operating parameters. The model is empirically based and provides a simple way to reach a definite conclusion based upon ''imprecise'' input information. The first step in

Table 1 Data validation

I, A	Ar + H_2, SLPM	H_2/Ar, %	Y_{exp}, μm	Y_{fuzzy}, μm	Difference, μm
350	54	35	4.08	4.70	0.62
440	54	35	5.33	6.08	0.75
530	54	35	6.82	6.43	−0.39
630	54	35	5.29	6.16	0.87
750	54	35	7.95	6.99	−0.96
530	30	35	7.16	6.98	−0.18
530	54	35	6.82	6.43	−0.39
530	40	35	7.66	6.40	−1.26
530	70	35	6.66	6.66	0.00
530	54	0	0.00	0.23	0.23
530	54	13	3.40	3.40	0.00
530	54	23	4.23	6.03	−1.80
530	54	33	5.14	6.43	−1.29
530	54	43	5.93	6.39	−0.46
530	54	50	6.39	6.32	−0.07

Y_{exp}: experimental deposition yield; Y_{fuzzy}: predicted deposition yield; difference: $Y_{fuzzy} - Y_{exp}$

implementing this concept is to decide exactly which parameters (inputs) have to be controlled and how.

3.1 Membership Functions

The membership function (MF) is a graphical representation of the magnitude of the contribution of each input (operating power parameters) on the considered result. It permits to (Ref 7):

- associate a weighting with each of the inputs that are processed;
- define functional overlap between inputs;
- determine ultimately an output response.

The rules use the input membership values as weighting factors to determine their influence on the fuzzy output sets of the final output conclusion. Once the functions are inferred, scaled, and combined, they are defuzzified into a crisp output which drives the system.

The parameters are decomposed into four types of input and output (Table 2), as follows (Ref 8):

- the *S membership function* (S). This spline-based curve is a mapping on the vector x, and is named because of its S-shape. The parameters for S membership function, a and b, locate the extreme values of the sloped portion of the curve;
- the *Z membership function* (Z). This spline-based function of the vector x is so named because of its Z shape. The parameters for Z membership function, a and b, locate the extreme values of the sloped portion of the curve which is expressed as follows:

$$\left\{\begin{array}{l} 1, x \le a \\ 1 - 2\left(\dfrac{x-a}{b-a}\right)^2, a \le x \le \dfrac{a+b}{2} \\ 2\left(\dfrac{b-x}{b-a}\right), \dfrac{a+b}{2} \le x \le b \\ 0, x \ge b \end{array}\right\} \quad \text{(Eq 1)}$$

- the *symmetric Gaussian membership function* (Gauss) which depends on two parameters, σ and c, as follows:

$$f(x, \sigma, c) = e^{-(x-c)^2/2\sigma^2} \quad \text{(Eq 2)}$$

- the *triangular membership function* (Tri). It is a function of the vector x and depends on three scalar parameters, a, b, and c, which locate the feet of the triangle (a and c) and its peak (b). All outputs MF are triangular. The function is expressed as follows:

$$f(x, a, b, c) = \max\left(\min\left(\frac{x-a}{b-a}, \frac{c-x}{c-b}\right), 0\right) \quad \text{(Eq 3)}$$

Fuzzy knowledge-base typically consists of three subprocesses: fuzzification, inference and defuzzification (Ref 9).

3.2 Fuzzification Step

The membership functions defined on the input variables are applied to their actual values to determine the degree of truth for each rule premise. This process aims at translating numerical values into linguistic descriptions (i.e., true, false, etc.). This is achieved by simply evaluating all the input MF with respect to the current set of input values in order to establish the degree of activation of each MF. At the end of this process, a list of activations is obtained and can be carried forward to the next stage (Ref 10).

3.3 Inference Method Step

The truth value for the premise of each rule is computed and applied to the conclusion part of each rule. The inference method which was applied in this study permits to test the magnitudes of each rule and select the highest one. The coordinate of the ''fuzzy centroid'' of the area under that function is taken as the output. This method does not combine the effects of all applicable rules but does produce a continuous output function and is easy to implement (Ref 11).

3.4 Defuzzification Step

This step aims at producing a quantifiable result in fuzzy logic. Characteristically, a fuzzy system will have a number of rules that transform a number of variables into a fuzzy result, that is to say that the result is described in terms of membership in fuzzy sets. The defuzzification method that was used is performed by combining the

Table 2 Power process parameters decomposition

	I [200-900]	$Ar + H_2$ [0-80]	H_2/Ar [0-60]
Null	MF: Z parameters: [300 300]	– –	MF: Z parameters: [10 15]
Very low	MF: Gauss parameters: [40 350]	MF: Z parameters: [10 20]	MF: Gauss parameters: [5 13]
Low	MF: Gauss parameters: [40 440]	MF: Gauss parameters: [5 30]	MF: Gauss parameters: [5 23]
Optimal	MF: Gauss parameters: [40 530]	MF: Gauss parameters: [5 40]	MF: Gauss parameters: [5 35]
High	MF: Gauss parameters: [40 630]	MF: Gauss parameters: [5 54]	MF: Gauss parameters: [5 43]
Very high	MF: S parameters: [530 750]	MF: S parameters: [54 70]	MF: S parameters: [45 50]

results of the inference process and then by computing the fuzzy centroid of the area (Ref 12). The weighted strengths of each output member function are multiplied by their respective output membership function center points and summed. Finally, this area is divided by the sum of the weighted member function strengths and the result is taken as the crisp output as follows:

$$\text{fuzzy output} = \frac{\int_U y\,\mu(y)\,dy}{\int_U \mu(y)\,dy} \quad \text{(Eq 4)}$$

where U represents all output values which are considered.

The Mamdani's method (Ref 13) which is based on the Zadeh's method (Ref 14) is applied in this study. A useful defuzzification technique must first add the results of the rules together in some way. The first step of defuzzification typically chops off the parts of the graphs to form trapezoids. Then, the centroid of this shape, called the fuzzy centroid is calculated. The coordinate of the centroid corresponds to the defuzzified value.

4. Results

To develop the fuzzy logic methodology, diverse steps are critical. These steps aim at:

- defining the control objectives and criteria, i.e., what must be done to control the system? What kind of response is needed? What are the system possible failure modes? etc.;
- determining the input and output relationships and selecting a minimum number of variables for input to the FL engine;
- using the rule-based structure of FL, splitting the control problem into a series of (for example) ''IF I AND $Ar + H_2$ AND H_2/Ar THEN WHAT'' rules that define the desired system output response for given system input conditions;
- generating FL membership functions that define the meaning (values) of Input/Output terms used in the rules;
- testing the system, evaluating the results, tuning the rules and membership functions, and retesting the system until satisfactory results are obtained.

4.1 Validation Step

For defined processing parameters, the deposition yield is mostly conditioned by the feedstock rate and the kinematics parameters (transverse gun velocity, scanning step, etc.) (Ref 15). Discriminating the effect of each power process parameter is important in order to control the process. Each power process parameter is divided into levels (Table 2) and each level is associated to one MF. These considerations permit to develop different combinations in order to determine the control rules.

The FL was computed to validate the relationships between power process parameters and the deposition yield. The results are summarized in Table 1. They are consistent with experimental data and the tolerance (difference) between experimental and fuzzy values permits to consider the system and such a methodology to predict operating parameters from required coating structural and/or mechanical attributes and to implement it to control the spray process.

4.2 Simulation Step

After model validation, the next step refers logically to the deposition yield prediction by fuzzy logic. Thus, acquired data permit to compute the deposition as a function of the power processing parameters. Table 3 displays the results.

Increasing arc current intensity leads to an increase in the fraction of the particle size distribution that forms the coating. As a result, the deposition yield increases. The same result is observed when considering the effect of the hydrogen fraction. Owing to thermodynamic constraints, the particle residence time within the plasma flow decreases as the plasma gas total flow rate increases. Indeed, when the gas flow rate increases from 50 SLPM to 80 SLPM, the fraction of the particle size distribution that forms the coating reduces and the deposition yield decreases.

Table 3 Deposition yield predicted by fuzzy logic system

I, A	$H_2 + Ar$, Nl min^{-1}	H_2/Ar, %	Y_{fuzzy}, µm
350	30	35	4.25
350	54	0	0.195
350	54	13	0.353
350	54	23	4.700
350	54	50	4.710
440	30	35	5.540
440	54	50	5.930
440	70	35	6.650
530	30	0	0.092
530	30	10	1.980
530	30	13	2.370
530	30	35	6.980
530	30	43	6.750
530	30	50	6.190
530	40	10	2.750
530	54	10	3.390
530	54	50	6.320
530	60	10	3.430
530	70	13	6.550
530	70	35	6.660
530	70	50	6.590
530	70	43	6.660
750	30	35	7.730
750	40	35	7.890
750	54	10	6.450
750	54	23	6.990
750	54	50	6.610
750	60	35	6.600

4.3 Effect of Power Process Parameters

Arc current intensity: Deposition yield presents a non-linear relationship *versus* the arc current intensity (Fig. 1). Nevertheless, from a general point of view, the arc current intensity increases the plasma energies (both enthalpy and momentum) (Ref 16). At a high power regime, that is to say at high arc current intensity, this increase is accompanied with a significant evaporation of particles. This is why at the highest current levels (higher than 600 A), the deposition yield variation is not significant anymore.

The polynomial (non-linear) relationship can be expressed as follows:

$$Y = (2E-07) \times I^3 - 0.0003 \times I^2 + 0.1843 \times I - 28.017, \quad R^2 = 0.9968 \qquad \text{(Eq 5)}$$

where Y [μm] is the deposition yield and I [A] represents the arc current intensity.

Plasma gas total flow rate: Deposition yield continuously decreases with the increase in the plasma gas total flow rate (Fig. 2). As the flow rate increases, the particle residence time within the plasma jet is reduced.

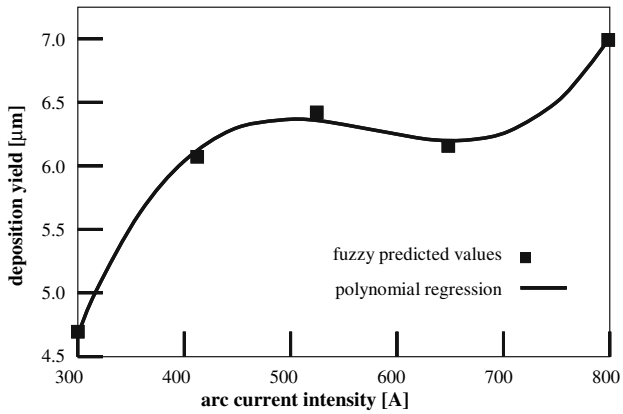

Fig. 1 Deposition yield evolution vs. arc current intensity ($V_{H_2+Ar} = 54$ SLPM and $V_{H_2/Ar} = 35\%$)

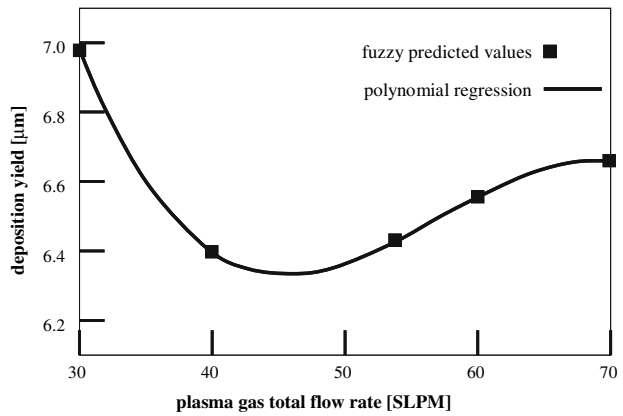

Fig. 2 Deposition yield evolution vs. plasma gas total flow rate ($I = 530$ A and $V_{H_2/Ar} = 35\%$)

This relationship can be expressed as follows:

$$Y = (-5E-05)(V_{H_2+Ar}^3) + 0.009(V_{H_2+Ar}^2) - 0.4991(V_{H_2+Ar}) + 15.191, \quad R^2 = 0.9999 \qquad \text{(Eq 6)}$$

where Y [μm] is the deposition yield and V_{H_2+Ar}[SLPM] represents the plasma gas total flow rate.

Indeed, the plasma flow rate increases the particles velocity and decreases their temperature in the plasma jet (Ref 16, 17). Consequently, the deposition yield decreases. Increasing the flow rate above a critical value leads to a decrease in the arc root diameter. Thus, only few particles will succeed in penetrating the reduced warm core region of the plasma jet. This is the major reason for which the deposition yield variation becomes insignificant for a total flow rate higher than 60 SLPM.

Hydrogen ratio: The correlation between the deposition yield and the hydrogen fraction is displayed in Fig. 3.

This operating parameter has a considerable effect on the deposition yield. Indeed, hydrogen ratio modifies the plasma jet characteristics (Ref 18), i.e., the plasma enthalpy, thermal conductivity and velocity increase while the plasma viscosity decreases.

The effect of this operating parameter can be expressed as follows:

$$Y = (7E-06)(V_{H_2/Ar}^4) - 0.0007(V_{H_2/Ar}^3) + 0.0169(V_{H_2/Ar}^2) + 0.1325(V_{H_2/Ar}) + 0.217, \quad R^2 = 0.9965 \qquad \text{(Eq 7)}$$

where Y [μm] is the deposition yield and V_{H_2+Ar}[%] represents the hydrogen ratio.

For low hydrogen fractions, the hydrogen still improves the thermal conductivity of the plasma jet and facilitates thermal exchange between the powder particles and the plasma jet. For high hydrogen ratios, deposition yield does not vary significantly due to the fact that the enthalpy of the plasma jet reaches a critical value inducing significant feedstock evaporation (Ref 19).

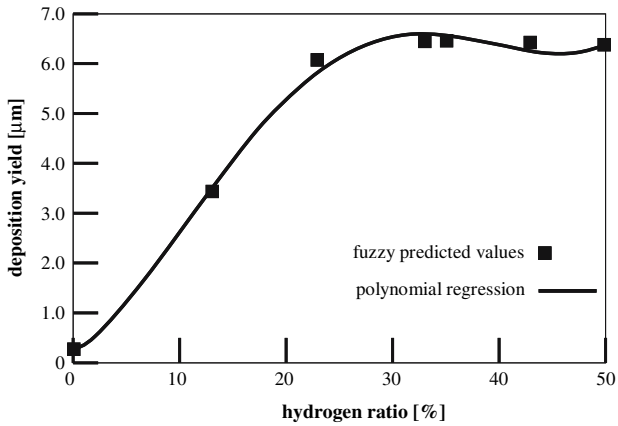

Fig. 3 Deposition yield vs. hydrogen ratio ($V_{H_2+Ar} = 54$ SLPM and $V_{H_2/Ar} = 35\%$)

5. Conclusion

Fuzzy logic model were implemented to determine the inter-relationships between power process parameters and coating structural (deposition yield) in plasma spray process. The proposed model is a convenient and powerful tool for practical optimization of the deposition yield and processing parameters in order to obtain the desired combination. These operating process parameters are strongly correlated together via mostly non-linear relationships. The model is open for constant upgrade and improvement.

Acknowledgment

LERMPS is a member of the *Institut des Traitements de Surface de Franche Comté* (ITSFC, Surface Treatment Instute of Franche Comté), France.

References

1. L. Pejryd, J. Wigren, D.J. Greving, J.R. Shadley, and E.F. Rybicki, Residual Stresses as a Factor in the Selection of Tungsten Carbide Coatings for a Jet Engine Application, *J. Therm. Spray Technol.*, 1995, **4**, p 268-274
2. H. Zhang, H.B. Xiong, and L.L. Zheng, Partially Melted and its Splat Morphology, *Thermal Spray 2003: Advancing the Science and Applying the Technology*, B.R. Marple and C. Moreau, Ed., May 5-8, 2003 (Orlanda, USA), ASM International, 2003, p 905-911
3. V. Srinivasan, A. Vaidya, T. Streibl, M. Friis, and S. Sampath, On the Reproducibility of air Plasma Process and Control of Particle State, *J. Therm. Spray Technol.*, 2006, **15**(4), p 739-743
4. M. Friis and C. Persson, Control of Thermal Spray Processes by Means of Process Maps and Process Windows, *J. Therm. Spray Technol.*, 2003, **12**(1), p 44-52
5. S. Guessasma, G. Montavon, and C. Coddet, Neural Computation to Predict In-flight Particle Characteristic Dependences from Processing Parameters in the APS Process, *J. Therm. Spray Technol.*, 2004, **13**(4), p 570-585
6. G. Montavon, C. Coddet, C.C. Berndt, and S.H. Leigh, Microstructural Index to Quantify Thermal Spray Deposit Microstructures Using Image Analysis, *J. Therm. Spray Technol.*, 1998, **7**(2), p 229-241
7. H. Sun and L. Liu, A Linear Output Structure for Fuzzy Logic Controllers, *Fuzzy Sets Syst.*, 2002, **131**(2), p 265-270
8. C.L. Chen, P.C. Chen, and C.K. Chen, Analysis and Design of Fuzzy Control System, *Fuzzy Sets Syst.*, 1993, **57**(2), p 125-140
9. S.O.T. Ogaji, L. Marinai, S. Sampath, R. Singh, and S.D. Prober, Gas-turbine Fault Diagnostics: A Fuzzy-logic Approach, *Appl. Energy*, 2005, **82**(1), p 81-89
10. M. Liang, T. Yeap, A. Hermansyah, and S. Rahmati, Fuzzy Control of Spindle Torque for Industrial CNC Machining, *Int. J. Mach. Tools Manuf.*, 2003, **43**(14), p 1497-1508
11. J.I. Horiuchi and M. Kishimoto, Application of Fuzzy Control to Industrial Bioprocesses in Japan, *Fuzzy Sets Syst.*, 2002, **128**(1), p 117-124
12. T Fraichard and P. Garnier, Fuzzy Control to Drive Car-like Vehicles, *Robot. Auton. Syst.*, 2001, **34**(1), p 1-22
13. E.H. Mamdani and S. Assilian, An Experiment in Linguistic Synthesis with a Fuzzy Logic Controller, *Int. J. Man-Machine Studies*, 1975, **7**(1), p 1-13
14. L.A. Zadeh, Outline of a New Approach to the Analysis of Complex Systems and Decision Processes, *IEEE Trans. Syst. Man Cybern.*, 1973, **3**(1), p 28-44
15. R. Kingswell, K.T. Scott, and L.L. Wassell, Optimizing the Vacuum Plasma Spray Deposition of Metal, Ceramic and Cermet Coatings Using Designed Experiments, *J. Therm. Spray Technol.*, 1993, **2**(2), p 179-185
16. M. Prystay, P. Gougeon, and C. Moreau, Structure of Plasma Sprayed Zircona Coatings Tailored by Controlling the Temperature and Velocity of the Sprayed Particles, *J. Therm. Spray Technol.*, 2001, **10**(1), p 67-75
17. M. Friis, C. Persson, and J. Wigren, Influence of Particle In-flight Characteristics on the Microstructure of Atmospheric Plasma Sprayed Yttria Stabilized ZrO_2, *Surf. Coat. Technol.*, 2001, **141**(2/3), p 115-127
18. E. Pfender, Fundamental Studies Associated with the Plasma Spray Process, *Surf. Coat. Technol.*, 1988, **34**(1), p 1-14
19. D.R. Marsh, N.E. Weare, and D.L. Walker, Process Variables in Plasma-jet Spraying, *J. Met.*, 1961, **2**, p 473-478